Journal of Sound and Vibration (2000) **232**(4), 659–668
doi:10.1006/jsvi.1999.2776, available online at http://www.idealibrary.com on IDEAL®

PROPOSITION OF A NEW APPROACH FOR THE SUBSTRUCTURE METHOD

H. HASSIS

Laboratoire Modélisation et Calcul de Structures LMCS, Ecole Nationale d'Ingénieurs de Tunis, B.P. 37, Le Belvédère 1002, Tunis, Tunisia

(*Received* 16 *November* 1998; *and in final form* 19 *August* 1999)

In this work a new projection basis for the substructure method is presented. This basis uses new correction solutions reducing the numerical of co-ordinates used in the dynamic analysis of a complex structure. For each connexion boundary, a "boundary structure" (whose characteristics are defined using a physical criterion) is associated. The correction solutions proposed here use the normal modes of the "boundary structure". On this basis, the size of problem and the compute time are reduced. Two structures are studied: a rectangular plate and the planetarium of the science city of Tunisia. The results show that the proposed method gives a good estimation of frequencies in comparison with the full finite element method results.

© 2000 Academic Press

1. INTRODUCTION

For a large system with many degrees of freedom (d.o.f.), it is very difficult and impractical to solve the equation of motion of the complete system directly. Hence substructure synthesis techniques have been used to evaluate the natural frequencies and mode shapes of large and complex structural systems. A complete structure is treated as an assemblage of substructures, and the motion of each substructure is represented by a set of substructure modes. Using equations of force equilibrium and compatibility between substructure interfaces, the substructures can be then coupled together.

Since Craig and Bampton's publication [1] several improvements of substructure synthesis methods have been proposed by Hale and Meirovitch [2], Wang and Chen [3], Leung [4] and Bourquin [5].

Gibert [6] reconsidered the method by using the impedance of a boundary. Chouieb and Hassis [7] presented a general formulation that takes into account the rigid-body modes, the impedance and the truncation of modes.

Jezequel *et al.* [8–10] presented a double-modal synthesis procedure. Generalized coordinates are introduced and force and displacement distributions applied along the boundary. This procedure introduces boundary d.o.f. associated with arbitrary boundary displacement shapes. The coupling of substructures has been taken into account in order to minimize the number of interface d.o.f.

In the same context, presented here is a substructure method synthesis using the response of the structure to the modes of a "boundary structure" associated with the boundary as correction solutions.

 © 2000 Academic Press

2. PRESENTATION OF THE PROPOSED NEW SUBSTRUCTURE METHOD

2.1. GENERALITIES

Refer to the overall structure S composed of substructures. The ith substructure S^i is limited by the boundary Γ^i. Γ^i is divided into three parts: Γ_u^i is the clamped part of the boundary, Γ_{F_i} is the part of the boundary where forces are imposed and Γ^{ik} is the substructure interface between the substructures S^i and S^k.

The material of the substructures is considered elastic and the dynamic problem is analyzed by considering a few perturbation hypotheses.

2.2. EQUILIBRIUM EQUATIONS OF A SUBSTRUCTURE S^i

For a substructure S^i, the dynamic equations for the ith substructure can be written as follows:

$$([\mathbf{K}] - \omega^2[\mathbf{M}])_{(i)} \cdot [\mathbf{U}]_{(i)} = [\mathbf{T}]_{(i)}, \tag{1}$$

where $\mathbf{K}$ and $\mathbf{M}$ are, respectively, the static stiffness matrix and the mass matrix of the substructure S^i. $\mathbf{U}$ denotes the displacements and $\mathbf{T}$ the applied forces on the substructure d.o.f.s. ω denotes the ith substructure frequency of vibration.

The d.o.f.s are grouped in terms of interface substructure d.o.f.s (denoted by B) and substructure non-interface d.o.f.s (denoted by I). Therefore, equation (1) can be written in partitioned form as follows:

$$\left(\begin{bmatrix} \mathbf{K}^{BB} & \mathbf{K}^{BI} \\ \mathbf{K}^{IB} & \mathbf{K}^{II} \end{bmatrix} - \omega^2 \begin{bmatrix} \mathbf{M}^{BB} & \mathbf{M}^{BI} \\ \mathbf{M}^{IB} & \mathbf{M}^{II} \end{bmatrix}\right)_{(i)} \cdot \begin{bmatrix} \mathbf{U}^B \\ \mathbf{U}^i \end{bmatrix}_{(i)} = \begin{bmatrix} \mathbf{T}^B \\ \mathbf{T}^i \end{bmatrix}_{(i)}. \tag{2}$$

2.3. PRESENTATION OF THE NEW PROJECTION BASIS

The new approach, like the Craig–Bampton approach, consists in developing the displacement $\mathbf{U}$ on the basis of the elastic modes of the substructure clamped at the interfaces Γ^{ik} and correction interfaces modes called correction solutions. The present approach proposes new correction solutions.

2.3.1. *Fixed-interface mode representation*

The fixed-interface normal modes of a substructure are determined by considering the free vibration of the substructure whilst the boundary d.o.f.s are constrained. The natural models $\boldsymbol{\psi}^{II}$, for clamped boundaries Γ^{ik}, can be written as

$$([\mathbf{K}^{II}] - \omega^2[\mathbf{M}^{II}])_{(i)} \cdot [\boldsymbol{\psi}^{II}]_{(i)} = 0. \tag{3a}$$

The normalized normal modes $\boldsymbol{\Psi}^{II}$ are defined by

$$\boldsymbol{\Psi}^{II} = \frac{\boldsymbol{\psi}^{II}}{\boldsymbol{\psi}^{II} \cdot \mathbf{M}^{II} \cdot \boldsymbol{\psi}^{II}}. \tag{3b}$$

2.3.2. *Correction solutions*

The correction solutions are introduced to reduce the clamped consideration effects used in the normal modes. Craig and Bampton proposed the following constraint modes: the constraint modes are considered from static considerations by applying a unit static displacement at each interface d.o.f.s in turn whilst all of the other interface d.o.f.s are constrained. The constrained mode shapes therefore describe the resulting displacement at each of the non-interface d.o.f.s. Let $[\boldsymbol{\psi}^s]$ denote the matrix whose column contains these constrained modes for the ith substructure. The expression of the constrained modes is

$$[\boldsymbol{\psi}^S]_{(i)} = \begin{bmatrix} \mathbf{I}^{SS} \\ \boldsymbol{\psi}^{SI} \end{bmatrix}_{(i)} \quad \text{with } [\boldsymbol{\psi}^{SI}]_{(i)} = -([\mathbf{K}^{II}]^{-1}[\mathbf{K}^{IS}][\mathbf{I}^{SS}])_{(i)}. \tag{4}$$

Note: The normal modes are generally normalized using the norm defined by equation (3b), but the Craig and Bampton correction solutions for a flexible structure can be greater than those for a rigid structure. Therefore, the matrices can be poorly conditioned and a numerical problem can be produced (see reference [9]).

The difference between the Craig and Bampton and the present approach is in the selection of the correction solutions. The correction solutions, proposed here, are considered from static–dynamic considerations by applying the function $\boldsymbol{\psi}^f$ as a static displacement of the interface boundary d.o.f.s. The functions $\boldsymbol{\psi}^f$ are defined by

$$([\mathbf{K}^f] - \omega^2[\mathbf{M}^f])[\boldsymbol{\psi}^f] = 0, \tag{5a}$$

where $[\mathbf{K}^f]$ and $[\mathbf{M}^f]$ are, respectively, the static stiffness matrix and the mass matrix of a structure called a "boundary structure". $\boldsymbol{\psi}^f$ represent the normal modes of the boundary structure.

The geometry of this boundary structure is the geometry of the boundary Γ^{ik}. The mechanical characteristics (E, Young's modulus, v, the Poisson ratio, A, cross-section, I, moments of inertia, etc.) of the boundary structure will be defined in Section 2.5. The *characteristics* of the boundary structure *must be correctly chosen in order to represent the motion of the substructure in the global structure.*

The normalized normal modes are defined by

$$\boldsymbol{\Psi}^f = \frac{\boldsymbol{\psi}^f}{\boldsymbol{\psi}^f \cdot \mathbf{M}^f \cdot \boldsymbol{\psi}^f}. \tag{5b}$$

The correction solutions are determined by applying $[\boldsymbol{\Psi}^f]$ at the interface boundary. The non-interface correction solutions $[\boldsymbol{\Psi}^{If}]$ can be expressed as

$$\begin{bmatrix} \mathbf{K}^{BB} & \mathbf{K}^{BI} \\ \mathbf{K}^{IB} & \mathbf{K}^{II} \end{bmatrix}_{(i)} \begin{bmatrix} \boldsymbol{\Psi}^f \\ \boldsymbol{\Psi}^{If} \end{bmatrix}_{(i)} = \begin{bmatrix} \mathbf{T}^f \\ \mathbf{0} \end{bmatrix}_{(i)} \Rightarrow [\boldsymbol{\Psi}^{If}]_i = -([\mathbf{K}^{II}]^{-1}[\mathbf{K}^{IB}][\boldsymbol{\Psi}^f])_{(i)}. \tag{6}$$

For our basis, the normal modes and the correction solutions are normalized by the same mass operator. In order to obtain well-conditioned matrices, criteria are proposed for the choice of mechanical and geometrical characteristics of the boundary structure (see Section 2.5). The dynamic substructure method has been developed in order to reduce the number of co-ordinates used in the dynamic analysis of complex problem. The size of the present correction solutions is smaller than Craig and Bampton's. The size of the global problem is

- *The present approach*: Number of normal modes $\times$ the number of substructure + number of boundary normal modes $\times$ the number of boundaries.
- *Craig and Bampton's approach*: Number of normal modes $\times$ the number of substructure + number of boundary d.o.f.s $\times$ the number of boundaries.

2.4. THE DEVELOPMENT OF THE DISPLACEMENT ON THE BASIS

For each substructure S^i, the displacement (in the global structure) is written as a development on the basis of the normal modes and the correction solutions:

$$[\mathbf{U}] = \begin{bmatrix} \mathbf{U}^B \\ \mathbf{U}^I \end{bmatrix} = \begin{bmatrix} \mathbf{\Psi}^f & \mathbf{0} \\ \mathbf{\Psi}^{If} & \mathbf{\Psi}^{II} \end{bmatrix} \begin{bmatrix} \boldsymbol{\beta}_f \\ \boldsymbol{\beta}_I \end{bmatrix} = [\boldsymbol{\psi}] \cdot [\boldsymbol{\beta}]. \tag{7}$$

As a consequence of such a transformation, the initial equations of motion (2) transform to

$$\{[\bar{\mathbf{K}}] - \omega^2 [\bar{\mathbf{M}}]\}_{(i)} \cdot \{\boldsymbol{\beta}\}_{(i)} = \{\bar{\mathbf{F}}\}_{(i)}, \tag{8}$$

where

$$[\bar{\mathbf{K}}] = [\mathbf{\Psi}]^{\mathrm{T}} [\mathbf{K}] [\mathbf{\Psi}] = \begin{bmatrix} \bar{\mathbf{K}}^{BB} & \mathbf{0}^{BI} \\ \mathbf{0}^{IB} & \bar{\mathbf{K}}_G \end{bmatrix}, \qquad [\bar{\mathbf{M}}] = [\mathbf{\Psi}]^{\mathrm{T}} [\mathbf{M}] [\mathbf{\Psi}] = \begin{bmatrix} \bar{\mathbf{M}}^{BB} & \bar{\mathbf{M}}^{BI} \\ \bar{\mathbf{M}}^{IB} & \bar{\mathbf{M}}_G \end{bmatrix},$$

$$[\bar{\mathbf{F}}] = \begin{bmatrix} \bar{\mathbf{F}}^B \\ \bar{\mathbf{F}}^I \end{bmatrix} = [\mathbf{\Psi}]^{\mathrm{T}} [\mathbf{F}].$$

Note that the orthonormality properties of normal modes give

$$\bar{\mathbf{K}}_G = \begin{bmatrix} \ddots & & \\ & \omega_n^2 & \\ & & \ddots \end{bmatrix}, \qquad \bar{\mathbf{M}}_G = \begin{bmatrix} 1 & & & & \\ & \ddots & & & \\ & & 1 & & \\ & & & \ddots & \\ & & & & 1 \end{bmatrix}.$$

2.5. EXAMPLE OF THE CHOICE OF BOUNDARY STRUCTURE CHARACTERISTICS

If the number of correction solutions is high, then the characteristics of the boundary structure do not have large effects because only the geometrical shape of the mode is important. But one of the advantages of this method is to reduce the size of the global problem by reducing the number of correction solutions.

Two criteria for the choice of the characteristics of the boundary structure are proposed here:

- The number of correction solutions must be "sufficient" to represent the real motion of the boundary.
- Matrices of the global problem must be well conditioned.

The boundary normal modes must contain transverse, longitudinal and torsional modes. This is easily obtained if all natural frequencies are in the same computational interval of frequencies. Take the example of a hinged plate ($L_1 \times L$) dividing into two parts (see Figure 1). A hinged–hinged beam is associated with the boundary between the two substructures of the plate. The characteristics of the boundary beam are: the cross-section A, the moment of inertia I and the tortional constant J. The first transverse frequency, f_f,

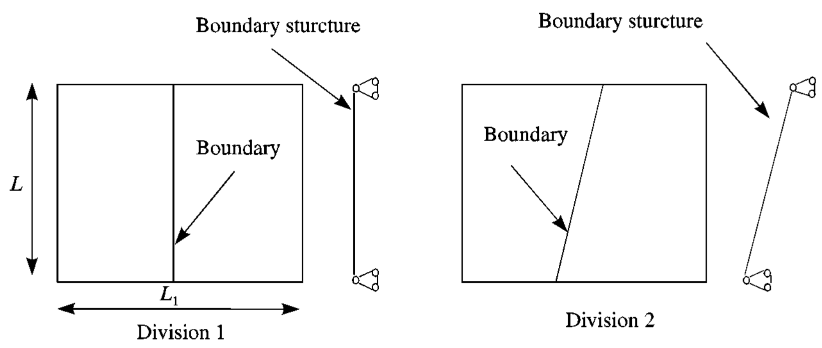

Figure 1. Subdivision of a plate in two substructures.

torsional frequency f_t and longitudinal frequency f_{tc} are

$$f_f = \frac{\pi}{2}\sqrt{\frac{EI}{\rho A}}\frac{1}{L^2}, \qquad f_t = \frac{1}{2L}\sqrt{\frac{G}{\rho}}, \qquad f_{tc} = \frac{1}{2L}\sqrt{\frac{E}{\rho}}. \tag{9a}$$

Using the first criterion $f_f \approx f_t = f_{tc}$, one obtains

$$\frac{1}{A} = \frac{L^2}{\pi^2}. \tag{9b}$$

By considering the second criterion, $f_f = (f_1)_{Plate}$, one obtains

$$\frac{EI}{\rho A} = (f_1)_{Plate}\frac{L^2}{\pi^4}, \tag{10}$$

where $(f_1)_{Plate}$ is the first frequency of the corresponding substructure.

To determine (A, I), one can impose a virtual section A and determine I. To determine (E, ρ), one can impose a virtual Young's modulus and determine ρ.

2.6. COUPLING TECHNIQUE

The coupling technique in this section is not new. Equation (8) is written for each substructure and the following linear connection relations between the substructures S^i and S^k are taken into account:

$$\{\mathbf{U}^B\}_{(i)} - \{\mathbf{U}^B\}_{(k)} = 0, \qquad \{\mathbf{F}^B\}_{(i)} + \{\mathbf{F}^B\}_{(k)} = 0. \tag{11}$$

3. APPLICATION

To show the implementation of the proposed basis, two substructures are chosen. The first structure is a rectangular plate and and second structure demonstrates the effectiveness of the method even when boundary is a curved line.

TABLE 1

Frequencies of the plate

Mode (Hz)	Frequency—Error		Frequency—Error		Frequency—Error	
F_{ad}	4·525	—	7·266	—	12·312	—
F_{nb1}	4·526	0·02%	7·265	0·01%	12·331	0·15%
F_{nb2}	4·585	1·32%	7·472	2·83%	12·872	4·54%

3.1. RECTANGULAR PLATE

The following results are derived for a rectangular plate with $L_1 = 20$ m by $L = 10$ m, and a thickness $h = 0{\cdot}20$ m (see Figure 1). The plate is hinged at the boundaries. The Young's modulus $E = 33 \times 10^9$ Pa, the mass density is $\rho = 2 \times 10^3$ kg/m^3 and the Poisson ratio $\nu = 0{\cdot}3$. The plate is divided in two substructures and two kinds of division are chosen, as shown in Figure 1. Table 1 gives the first three natural frequencies obtained with this new basis, compared to the full finite element method results.

F_{ad} is the natural frequencies obtained using a full finite element method (FEM). F_{nb1} and F_{nb2} are, respectively, the natural frequencies associated to the first and the second types of division.

The size of the correction solutions is equal to:

- 66 (1 boundary $\times$ 11 nodes $\times$ 6 d.o.f.s) for the Graig and Bampton method;
- 6 (6 normal boundary modes $\times$ 1 boundary) for the new basis.

A good estimation of frequencies is obtained by comparison with the full finite element method (with the same discretization).

3.2. COUPLED SHELLS–PLATES WITH CURVED BOUNDARIES: THE PLANETARIUM OF THE SCIENCES CITY OF TUNIS (TUNISIA)

The planetarium of the sciences city of Tunis (Tunisia) is composed of a spherical shell (with a diameter equal to 20 m) with three circular plates, representing the three stories. A cylindrical shell, representing the escalator, passes through the three circular plates. The first substructure is the spherical shell and the second substructure is made up of the three circular plates and the cylindrical shell (see Figure 2).

The boundary structures are three circular beams associated with the circular connection between the spherical shell and the circular plates. The modes used are the six rigid-body modes and four deformation modes for each circular beam.

The first three frequencies obtained by the full finite element method and the present approach are given by Table 2.

The first and the third mode shapes, obtained through out approach, are shown in Figure 3. The number of correction solution is

- 144 (3 boundaries $\times$ 8 nodes $\times$ 6 d.o.f.s) for the Craig and Bampton method;
- 12 (4 modes $\times$ 3 boundaries) for the present basis.

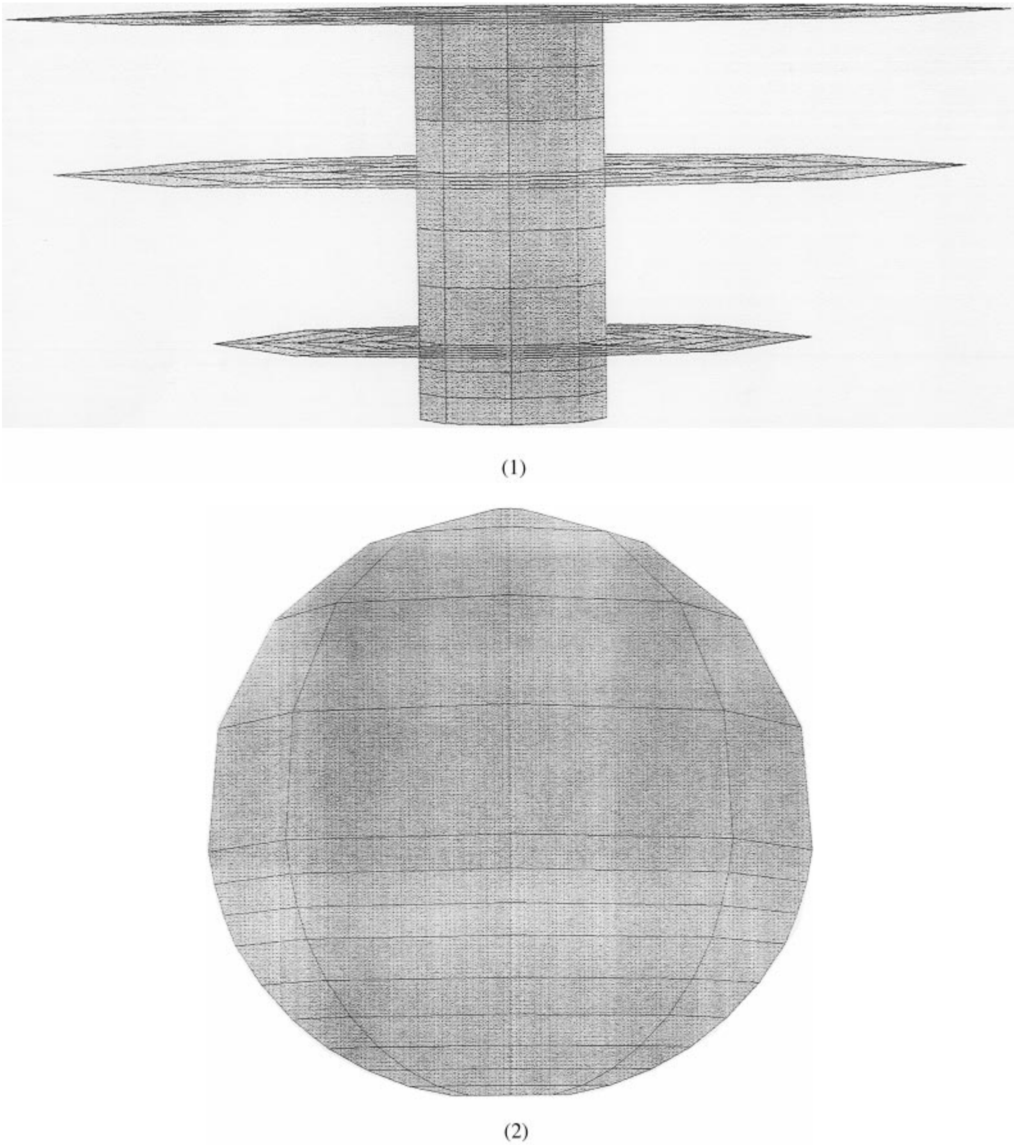

Figure 2. Substructure of planetarium of sciences city of Tunisia. Substructure 1: a cylindrical shell with three plates. Substructure 2: Spherical shell.

TABLE 2

Frequencies of planetarium

Mode (Hz)	Frequency	Error	Frequency	Error	Frequency	Error
F_{ad}	4·189	—	4·189	—	11·285	—
F_{nb}	4·478	6·9%	4·478	6·9%	11·046	2·1%

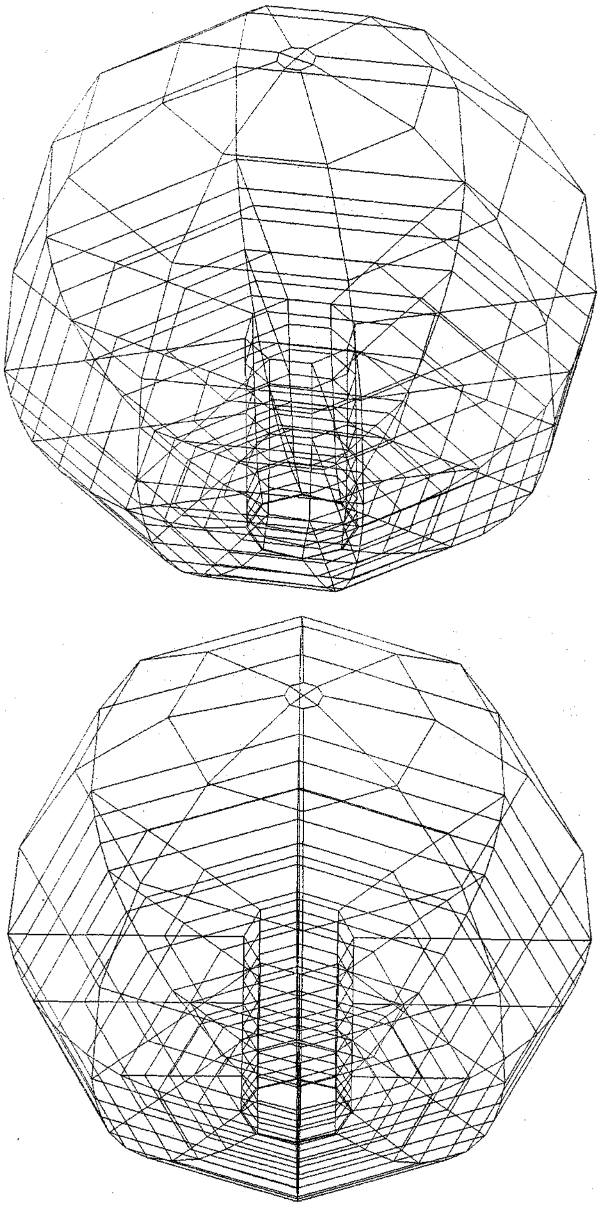

Figure 3. The first and the third mode shape of the planetarium of science city of Tunis, obtained by using the new approach.

4. CONCLUSION

To improve the modelling of each substructure in dynamic synthesis, a new basis has been developed. The proposed new basis uses new correction solutions. Such correction solutions are determined by applying the normal modes of the associated boundary structure to the interface boundary. The characteristics of the boundary structure are defined by using specific criteria.

The new approach is applied to two cases: a rectangular plate and the planetarium of the sciences city of Tunis (Tunisia). The results show that the proposed approach gives good estimation of frequencies and has significant computational advantage in comparison to the Craig and Bampton method, mainly in reducing the size of global problem.

N.B.: CASTEM 2000 code of C.E.A. France is used for the computational results.

REFERENCES

1. R. Craig and M. Bampton 1968 *AIAA Journal* **6**, 1313–1321. Coupling of substructures for dynamic analysis.
2. A. L. Hale and L. Meirovitch 1982 *Journal of Sound and Vibration* **84**, 269–287. A general procedure for improving substructures representation in dynamic synthesis.
3. J. H. Wang and H. R. Chen 1988 *Computer Methods in Applied Mechanics and Engineering* **79**, 203–217. A substructure modal synthesis method with high computational efficiency.
4. A. Y. Leung 1991 *Journal of Sound and Vibration* **149**, 83–90. Dynamic substructure response.
5. F. Bourquin and R. Namar 1997 *3ème colloque National en Calcul des structures*. Cinématique de l'interface en sous structuration dynamique.
6. R. J. Gibert 1988 *Collection de la direction des ètudes et recherches d'èlectricitè de France. Eyrolles*. Vibration des structures.
7. N. Chouieb and H. Hassis 1995 *5 ème colloque Maghrébin sur les Modèles Numèriques de l'Ingènieur* 21 *au* 23 *Novembre*. Sous structuration dynamique. Prise en compte de l'impédance, de modes rigides et de la troncature de la basis.
8. L. Jezequel and S. T. Tchere 1991 *Journal of Sound Vibration* **144**, 409–419. A procedure for improving component-mode representation in structural dynamic analysis.
9. L. Jezequel and H. D. Setio 1994 *Journal of Applied Mechanics* **61**, 109–116. Component modal synthesis methods based on hybrid models. Part I: theory of hybrid models and modal truncation methods.
10. L. Jezequel and H. D. Setio 1994 *Journal of Applied Mechanics* **61**, 109–116. Component modal synthesis methods based on hybrid models. Part II: numerical tests and experimental identification of hybrid models.

APPENDIX: NOMENCLATURE

A	cross-section
E	Young's modulus
f_t	torsional frequency
F_{ad}	natural frequencies obtained using a full finite element method (FEM)
h	thickness of the plate
J	torsional constant
$\mathbf{K}^f$	stiffness matrix of the "boundary"
$\mathbf{M}^f$	mass matrix of the "boundary"
S^i	ith substructure
$\mathbf{U}$	displacement vector
Γ_u^i	clamped part of the boundary
Γ^{ik}	interface between Γ^i and Γ^k
ω	radian frequency
$\mathbf{\Psi}^{II}$	unitary normal modes
v	the Poisson ratio
d.o.f.s	degrees of freedom
f_f	first transverse frequency
f_{tc}	longitudinal frequency
F_{nbi}	nth natural frequencies associated with the ith type of division
I	moment of inertia
$\mathbf{K}$	static stiffness matrix
$\mathbf{M}$	mass matrix
S	overall structure S

$\mathbf{T}$	applied forces on S^i
Γ^i	boundary of S^i
Γ^i_F	part of the boundary where forces are imposed
$\boldsymbol{\psi}^{II}$	natural modes for clamped boundaries Γ^{ik}
ρ	the mass density